Support Information

Surface-deprotonated ultra-small SnO_2 quantum dots for high-performance perovskite solar cells

Wuchen Xiang[‡1,3], *Yiheng, Gao*[‡1], *Bobo Yuan*[1], *Shuping Xiao*[1], *Rui Wu*[1], *Yiran, Wan*[1], *Zhiqiang Liu*[3], *Liang Ma*[1], *Xiangbai Chen*[1], *Weijun Ke*[2], *Guojia Fang*[2], *Pingli Qin**[1]

Mr W. Xiang, Mr Y. Gao, Mr B. Yuan, Ms S. Xiao, Ms R. Wu, Mr Y. Wan, Dr L. Ma, Prof. X. Chen, Prof. P. Qin

[1] Hubei Key Laboratory of Optical Information and Pattern Recognition, Wuhan Institute of Technology, Wuhan, Hubei 430205, P. R. China

Prof. W. Ke, Prof. G. Fang

[2] School of Physics and Technology, Key Laboratory of Artificial Micro- and Nano-structures of the Ministry of Education and School of Physics and Technology, Wuhan University, Wuhan 430072, P. R. China

Dr, Z. Liu

[3] Wuhan National Laboratory for Optoelectronics and School of Optical and Electronic Information, Huazhong University of Science and Technology, Wuhan, 430074, P. R. China

‡These authors contributed equally to this article.

*Corresponding author

E-mail: qpl2015@wit.edu.cn

This Supplementary Information includes:
Supplementary Figures 1 to 17
Supplementary Tables 1 to 3

Experimental Section

Materials.

Fluorine-doped tin oxide (FTO, 14 $\Omega \cdot sq^{-1}$) were supplied from Asahi Glass (Japan).Tin chloride dehydrates ($SnCl_2 \cdot 2H_2O$, 99.99%), thiourea ($SC(NH_2)_2$, 99.0%), Dimethyl sulfoxide(DMSO, 99.9%), N,N-Dimethylformamide(DMF, 99.9%), acetonitrile, Chlorobenzene (CB, 99.9%) and CsI (99.99%) were purchased from Sigma-Aldrich, While tripotassium citrate monohydrate and iso-Propyl alcohol (IPA, 99.75%) was bought from Sinopharm Chemical Reagent Co., Ltd. Formamidinium iodide (FAI) was bought from Great cell Solar Australia Pty., Ltd. PbI_2 (99.8%) was purchased from Tokyo chemical industry CO., LTD. while Spiro-OMeTAD (99.5%) was purchased from Shenzhen Feiming Science Technology Co. Ltd. 4-tert-butylpyridine (TBP, 96%), $PbBr_2$ (99.99%) and bis (trifluoromethane) sulfonimide lithium salt (Li-TFSI, 99%) were purchased from Xi'an Polymer Light Technology Corp. All aqueous solutions were freshly prepared using double-distilled water.

SnO_2-None synthesis

Different weight $SnCl_2 \cdot 2H_2O$ was slowly added into 30 mL of deionized water. After vigorously stirring in air ambient for 24h, a clear and transparent yellow SnO_2 quantum dots (QDs) solution was obtained.[1, 2] Noting, it is required that stirred magneton must be kept the dynamic balance to avoid water solvents escaping from the hydrolysis process. After filtration with a 0.22um filter, the SnO_2 QDs solution can be used to prepared electron transport layer. The possible hydrolysis-oxidation (containing

hydrolysis, dehydration and oxidation) process as followed:

$$SnCl_2{\cdot}2H_2O \xrightarrow{Hydrolysis} Sn(OH)Cl + HCl\#(1)$$

$$Sn(OH)Cl + H_2O \xrightarrow{Hydrolysis} Sn(OH)_2 + HCl\#(2)$$

$$Sn(OH)_2 + O_2 \xrightarrow{Dehydration\ and\ Oxidation} SnO_2 + H_2O\#(3)$$

Solution preparation: The $FA_{0.95}Cs_{0.05}PbI_{2.7}Br_{0.3}$ precursor solution was prepared in a glovebox from 1.38 M Pb^{2+} in a mixed solvent of DMF and DMSO (4:1 v/v), and then stirred at 39°C for 4 h to prepare perovskite precursor solution. Spiro-OMeTAD solution was prepared by dissolving 72.3 mg of spiro-OMeTAD, 29 μL of TBP and 17.5 μL of Li-TFSI solution (520mg mL^{-1} in acetonitrile) in 1ml CB.

Photocatalytic hydrogen production test: The hydrogen production performance of the prepared SnO_2 QDs samples were tested under simulated solar light from a 300W Xe arc lamp (Beijing China Education Au-Light Co., Ltd.) with a 420 nm cut filter. Here, SnO_2 QDs were deposited on fluorine-doped tin oxide (FTO), and then put into a glass reaction vessel with quantified deionized water. Generally, 22 mg of the prepared photocatalyst was dispersed in 80 mL of a mixed aqueous solution of 0.35 mol L^{-1} Na_2S and 0.25 mol L^{-1} Na_2SO_3. Finally, the amount of H_2 produced was measured by using a gas chromatograph (GC) equipped with a thermal conductivity detector (TCD) at different times.

Device Fabrication

First, FTO substrates were soaked in hot water with detergent for 20 min, and then ultrasonically treated in deionized water, acetone, and IPA solution successively, then

dried in the oven at 60°C for 8 hours. After these FTO substrates were treated in UV-ozone for 15 minutes, SnO_2 colloidal solution was spin-coated and casted at different spin-speed for 30 s and annealed at 180 °C for 1 h in air ambient. After cooling down, the prepared perovskite precursor solution was spin-coated and casted on SnO_2 at a speed of 4000 rpm for 30 seconds by the anti-solvent method in an Ar-filled glovebox. Note that 180 μL of CB solution was pipetted onto the spinning film at 10 s before the end of this program. Thereafter, the as-cast perovskite film was annealed at 100°C for 1 hour. After cooling down, the spiro-OMeTAD solution was spin-coated and casted for 30 s at a speed of 4000 r/min. Finally, Au was deposited on spiro-OMeTAD layer by thermal evaporation to complete the device, and the electrode is patterned using a shadow mask. The active area of the perovskite solar cells is 0.09 cm^2, which is defined by the area of the Au electrode.

Device Characterization

HR-TEM (FEI Titan G2 60-300) was used to detect the crystal plane spacing of SnO_2 QDs.

The simultaneous TG-DSC measurements were carried out with a DSC 21400A12. system under nitrogen atmosphere. Throughout this study, the flow of nitrogen gas was fixed at 30.0 mL/min. The heating rate has been studied at 10℃/min, using approximately 10 mg powdered samples contained in a platinum crucible. α-Al_2O_3 is used as a reference material.

XRD patterns were collected on an X-ray diffraction meter (XRD, Bruker AXS,

D8 Advance) with Cu Kα radiation (λ=0.1540 nm) and a graphite monochromator under operation conditions of 40 kV and 40 mA. The scan range (2θ) was from 10 to 90° with a step of 0.08° and scan speed of 5.00°/min.

XPS spectra were performed using an XPS/UPS system (Thermo Scientific, ESCLAB 250Xi, USA). All the films were sputtering-cleaned to remove atmospheric contamination in the XPS chamber for approximately 20 s by lower energy of Ar^+, and the Ar^+ gun was operated at 0.5 kV at a pressure of 1×10^{-7} Pa. The vacuum pressure of the analysis chamber was better than 2×10^{-8} Pa. For XPS, survey scans to identify overall surface composition and chemical states were performed using a monochromated Al Kα X-ray source ($h\upsilon$=1486.68 eV), detecting photoelectrons at 150 eV pass energy and a channel width of 500 meV. High-resolution scans to identify bonding states were performed at 20 eV pass energy and 50 meV channel width. The surface carbon signal at 284.6 eV was used as an internal standard. The XPS spectra were fitted by Gaussian-Lorentzian curves to obtain the relative contents of the various valence states.

FTIR spectrum was recorded with a reflectance instrument (Nicolet 6700, USA) from 4000 to 800 cm^{-1} with a resolution of 2 cm^{-1}.

Raman spectroscopy was measured by 633 nm laser (Thermo Scientific, USA).

UV–vis spectroscopy was performed using a UV–vis–NIR spectrophotometer (Tu-1810) in the 200–900 nm wavelength range at RT.

The thickness of films was measured through a step profiler (KLA-Tencor, D-300).

A high-resolution field emission scanning electron microscope (SEM, GeminiSEM 300) was used to observe the morphology of perovskite films and SnO_2 QDs/FTO. Meanwhile, the morphology of SnO_2 QDs/FTO was characterized by atomic force microscopy (AFM SPM-9500 J3, Shimadzu, Japan) with the contact mode (scanning tip: single-crystal Si_3N_4, spring constant: 0.02 N m^{-1}).

Using generalized gradient approximation Becke-Lee-Yang-Parr- (GGA-BLYP) density functional theory, The Geometry Optimization relaxation and structure optimization of the SnO_2 structure calculated by using the DMol3 module in Materials Studio. The charge density and electrostatic potential are described by DNP 4.4 basis set. The convergence criteria for energy force and displacement are $2x10^{-5}$ Ha, 0.004 $HaÅ^{-1}$ and 0.005 Å, respectively. The electron self-compatible field (SCF) tolerance is set to 10^{-5} Ha, and the maximum SCF self-consistent field cycles is 500. The adsorption energy (E_{ads}) is calculated as follows: $E_{ads}=E_{Groups}+E_{Surface}-E_{Groups/surface}$,[3, 4] where E_{Groups} is the total energy of an isolated molecule (or groups), $E_{Surface}$ and $E_{Groups/surface}$ are the total energy of the various SnO_2 (110) surfaces without and with molecule (or groups) adsorption respectively.

The J–V characteristics of the devices were measured using a B1500 A semiconductor parameter analyzer under an AAA class Oriel Sol3A solar simulator equipped with an AM 1.5G filter. The light intensity was set at 100 $mW·cm^{-2}$ using a standard Newport monocrystalline Si reference cell traceable to NREL calibration. The J–V scanning was done at a scan rate of 0.05 $V·s^{-1}$. The scans start and finish under forward bias and have 2 s stabilization time at forward bias under illumination prior to

scanning.

The steady-state PCE as a function of time was set at a fixed voltage of the maximum power point on the J-V curve (reverse scan, from open circuit to short circuit).

The corresponding IPCE spectra were measured by a QE/IPCE system (Enli Technology Co., Ltd.) in the 320–800 nm wavelength range at room temperature.

FTIR spectrum was recorded with a reflectance instrument (Nicolet 6700, USA) from 4000 to 800 cm^{-1} with a resolution of 2 cm^{-1}.

The steady-state PL spectrum and TRPL decay spectra (HORIBA Jobin Yvon IBH Ltd.) were observed with a 481 nm laser. PL measurements were obtained at several locations on the perovskite samples with 481nm CW excitation from the film side (laser spot size of ~140 μm, integration time of 0.5 s, laser intensity of 140 mW/cm^2) at room temperature. The PL signal was detected with a Symphony II CCD detector (Horiba) after a 300 g/mm grating monochromator. TRPL measurement at different locations of the samples was performed with a time correlated single photon counting module (Becker & Hickel Simple Tau SPCM 130-E/M module). A 481nm pulsed laser (beam diameter of ~100 μm) was used as a source of excitation. Samples were excited with ~10^{10} photons/pulse/cm^2 at the peak emission wavelength, as determined from the PL measurement. The PL signal was detected by PMT hybrid detector after a Horiba IHR 320 monochromator (900 g/mm, 850 nm blaze) grating. Decay curves were fitted to a biexponential decay function to analyze the carrier extraction at the perovskite/PFSA or PEDOT:F, which was fitted by an empirical double exponential model:[5]

$$y=A_1\exp(-t/\tau_1)+A_2\exp(-t/\tau_2)+y_0$$

Where y_0 is the attenuation constant, A_1 and A_2 represent the attenuation amplitude of photoluminescence, τ_1 refers to the rapid decay process from quenching of trap states or interfacial charge transfer, τ_2 is a slow decay process caused by interfacial non-radiative recombination.[6]

TPLM measurements were performed on home-built PL-scanned imaging microscopy coupled with time-correlated single-photon counting. The 405 nm wavelength (PIXEA405, Aurea Technology, France) excitation laser beam was focused on the sample through a 100× air objective lens (NA=0.95, Olympus PLFLN 100×). Fast scanning of the galvanometer mirror was used to collect photons emission from the $CsEuBr_3$ film. The 100× air objective lens was used to form an excitation spot of tens of micrometers in diameter, and then the excitation laser beam was uncollimated. Each scanning image contains 256×256 pixels. Two high-speed detectors (HPM-100-50 and HPM-100-40, Hamamatsu, Japan) were used to collect the fluorescence signal, and the optical filters in our measurements were 440–480 nm.

Space-charge-limited-current analysis is utilized to conduct a deep analysis on the micro-mechanism the surface/grain boundaries defects related to the perovskite film. The electron trap state density (n_{trap}) can be calculated by the twist point of the linear ohmic response and the fast exponential response. The trap filling limit voltage (V_{TFL}) at the kink point can be calculated by the formula n_{trap}: $V_{TFL}= e\, n_{trap}\, L^2/2\varepsilon\varepsilon_0$, therein, V_{TFL} is the trap filling voltage, e is the basic charge, n_{trap} is the trap density, L is the

thickness of perovskite film, ε and ε_0 are the relative dielectric constant and vacuum dielectric constant respectively.

The EIS was acquired on an electrochemical workstation (chi660d, China) in dark. Nyquist curves can be divided into two parts: The high-frequency component is related to the charge-transport resistance (R_{TR}) and the transport chemical capacitance (C_{TR}) property between the cathode and the anodes; and the low frequency component is assigned to the recombination resistance (R_{REC}) and the recombination chemical capacitance (C_{REC}) feature in the perovskite solar cells. Besides, series resistance (R_s) is correlated to internal series resistance of some layers except the perovskite sandwich structure in the device, such as FTO layer.

The unencapsulated devices were stored in a dry and dark box (~70% humidity at 20-25°C) for the stability tests. The un-encapsulated devices were put under a 150 W white light-emitting diode (wLED) flood light for testing of photo degradation, with 0.8-sun illumination (evaluated by standard KG5 Si diode).

X-ray characterization was performed using a medical X-ray tube (Leo, Varex imaging). The X-ray source operated at 50 kV voltage, and the X-ray spectrum was adjusted by adding 0.3 mm thick Cu plate and 1 mm thick Al plate to meet the RQA3 standard. The tube current is adjusted at 25 mA. The X-ray response of the devices was recorded using a semiconductor parameter analyzer (PRIMARIUS, FSPro).

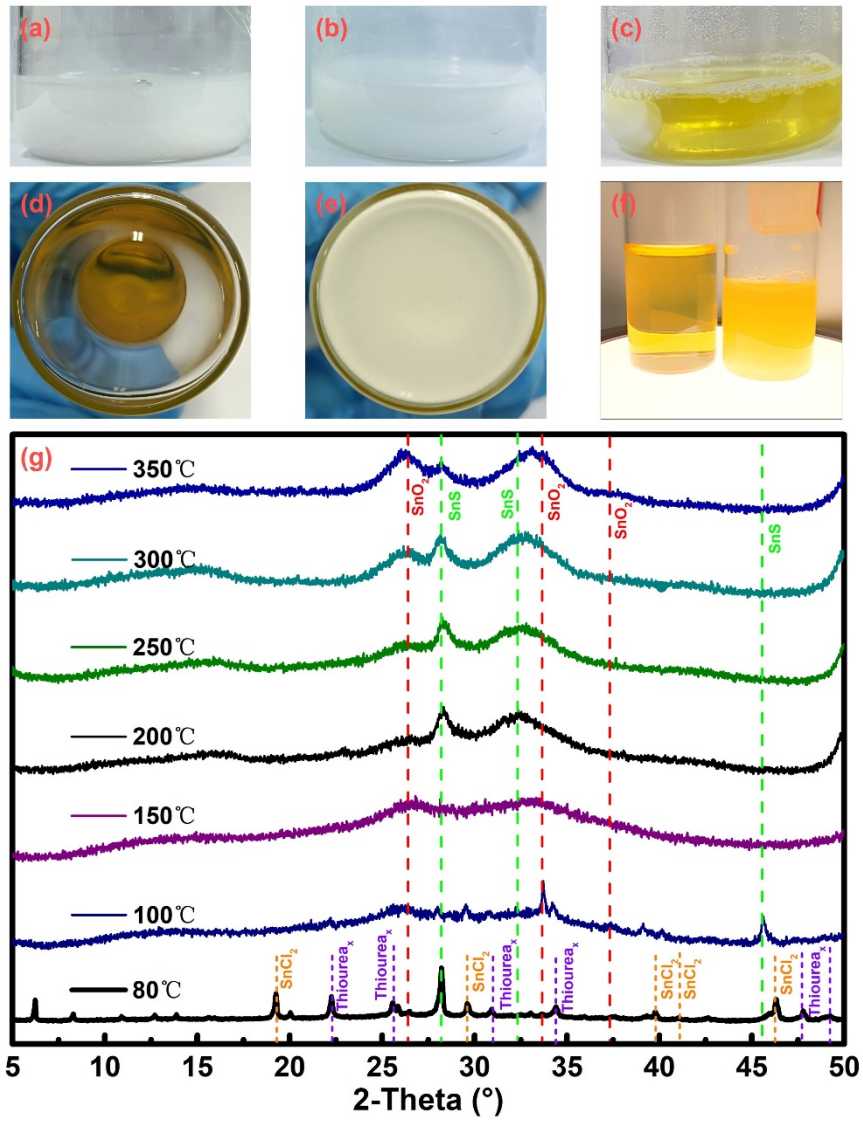

Fig. S1 Time dependent image of SnO_2 synthesis. (a) the dispersion of $SnCl_2 \cdot 2H_2O$ into deionized water and the reaction for (b) 5 & (c) 24 hours. The bottle bottom images of (d) SnO_2 QDs-N and (e) SnO_2 QDs-T water solution aged for a month, and (f) illumination images with them oscillated violently: the SnO_2 QDs-N water solution was located at left and the SnO_2 QDs-T based water solution was located at right. (g) XRD patterns of the white precipitates with annealed at different temperature.

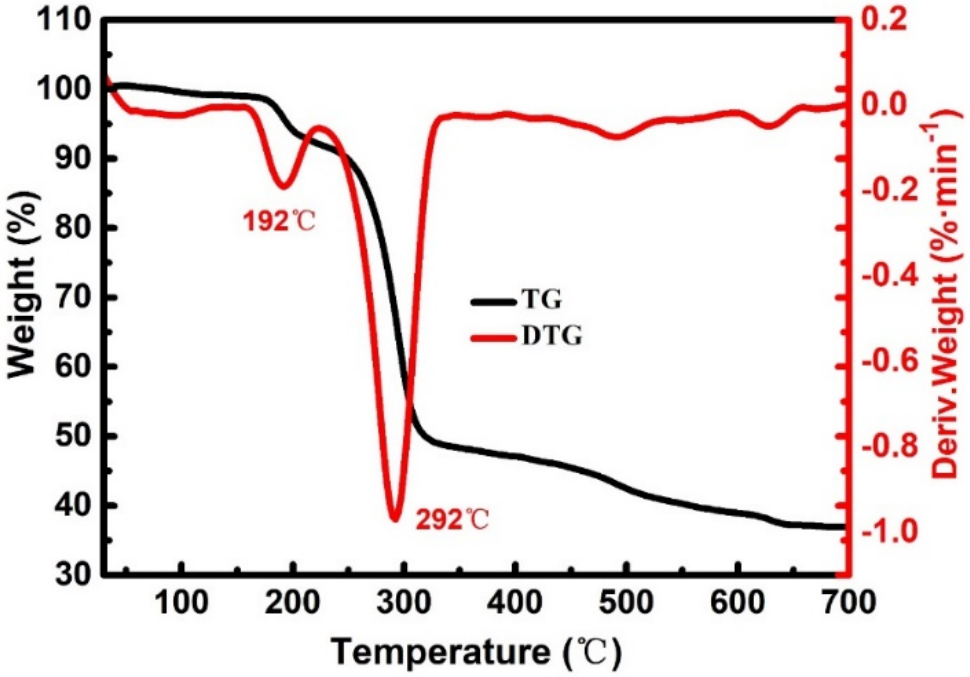

Fig. S2 TG and DTG curves of Thiourea.

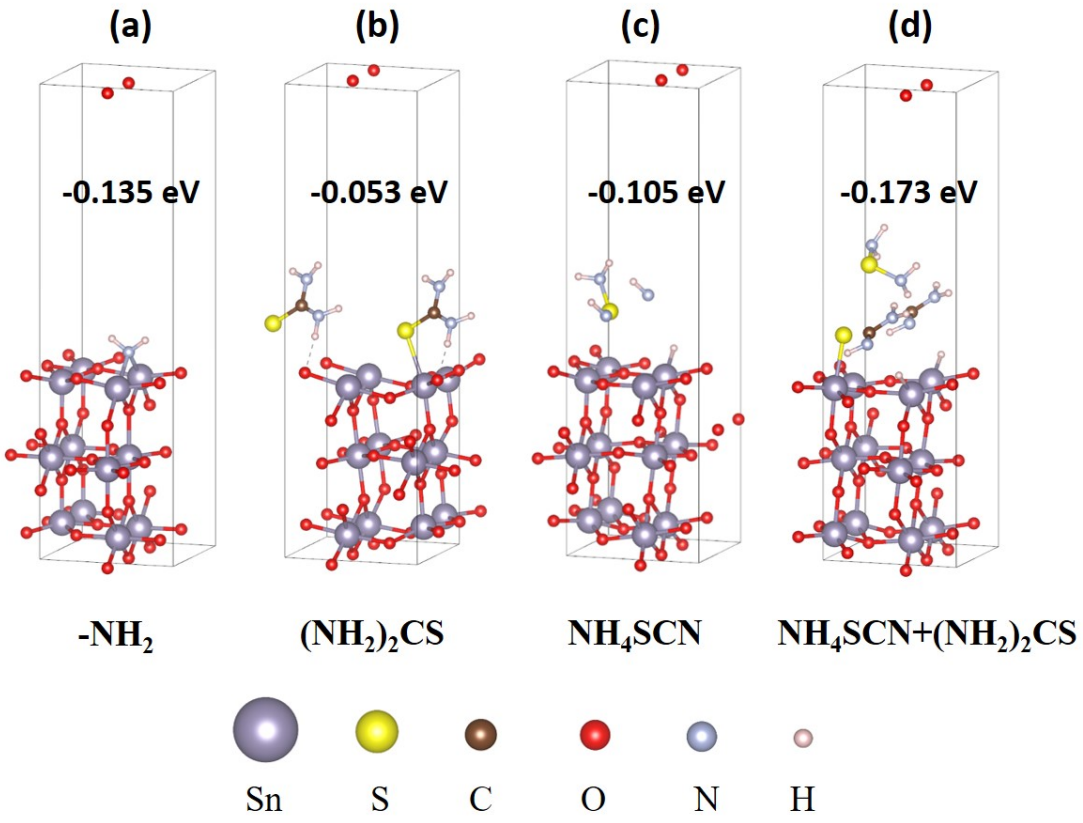

Fig. S3 Surface adsorption energy. (a) -NH_2 groups, (b) $(NH_2)_2CS$, (c) NH_4SCN and (d) NH_4SCN+$(NH_2)_2CS$ on the (110) surface of SnO_2 QDs.

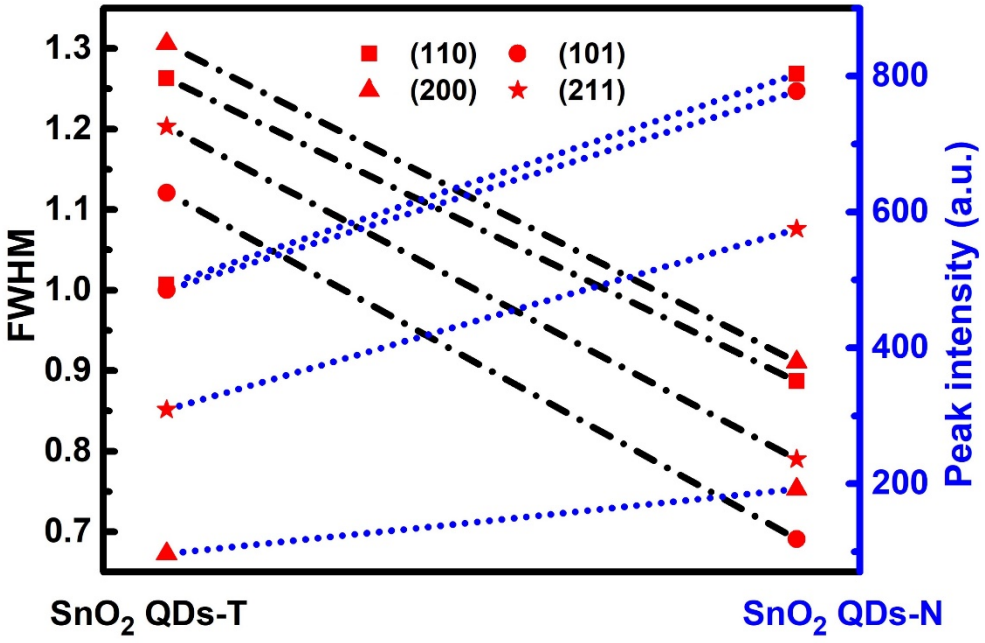

Fig. S4 Peak intensity and the corresponding FWHM for the diffraction peaks.

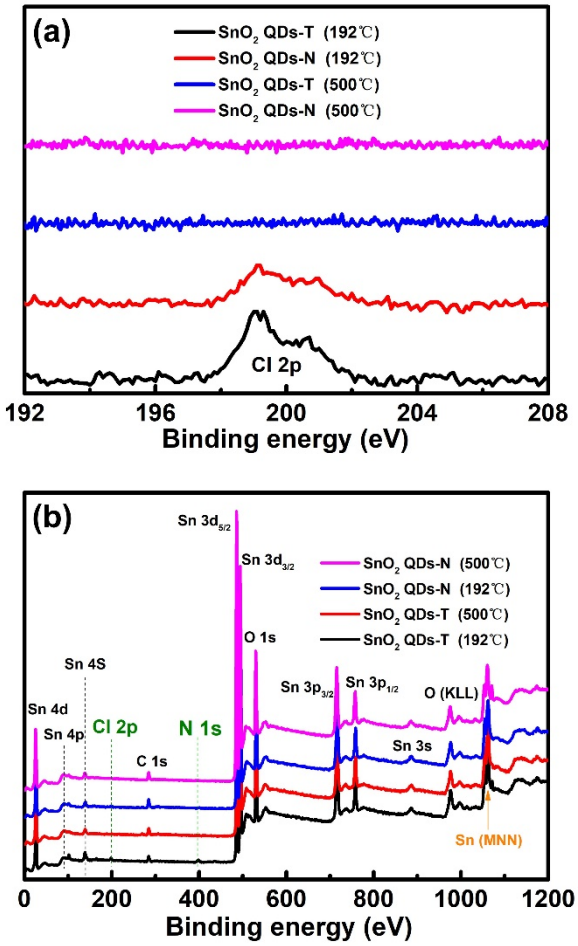

Fig. S5 XPS spectra. (a) Cl 2p and (b) survey for SnO_2 QDs films.

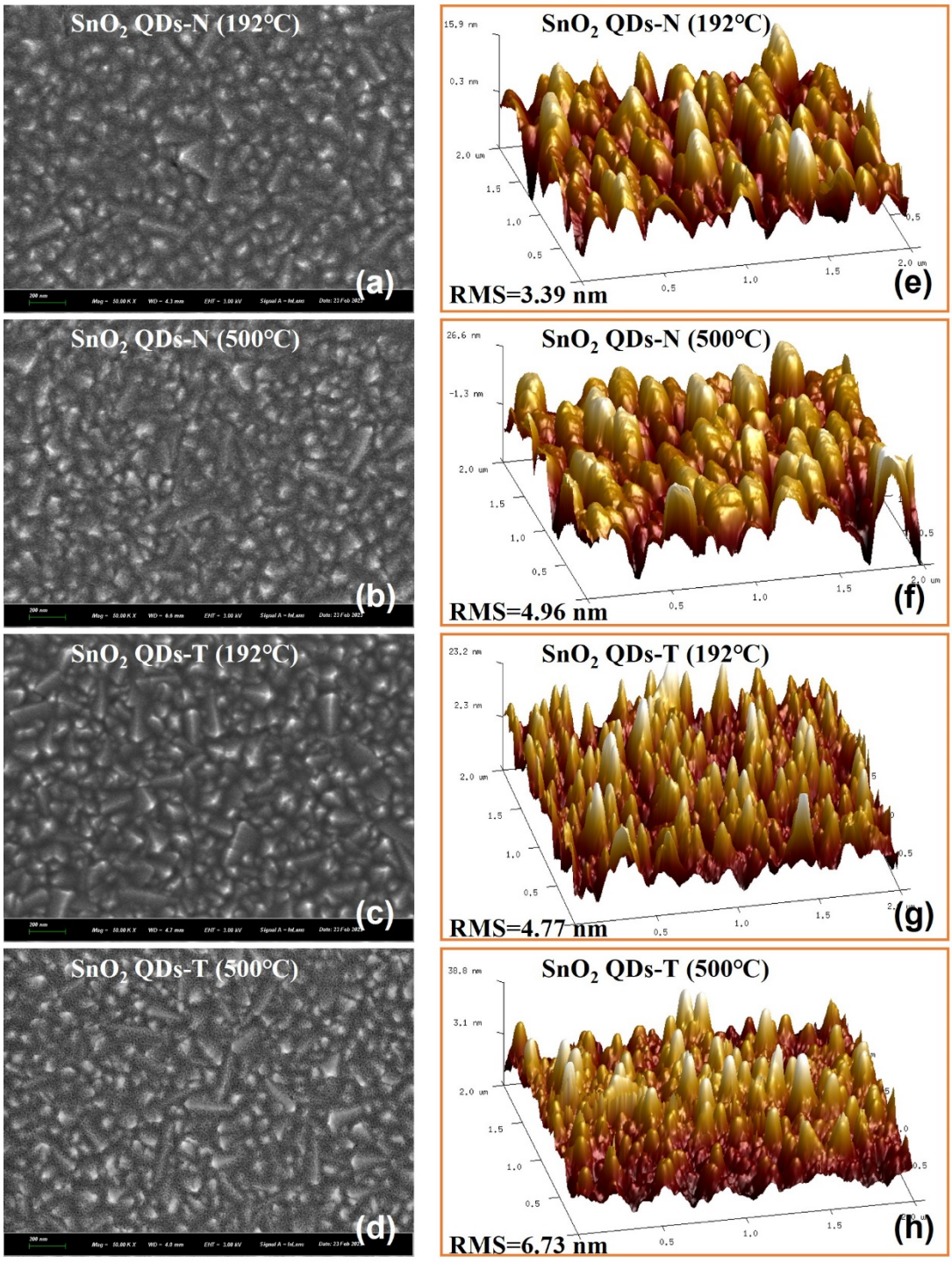

Fig. S6 SEM and AFM images. SnO_2 QDs-N (a, b, c, and d) and SnO_2 QDs-T (e, f, g, and h). SEM and AFM images were obtained from the samples with SnO_2 QDs deposited on an FTO substrate.

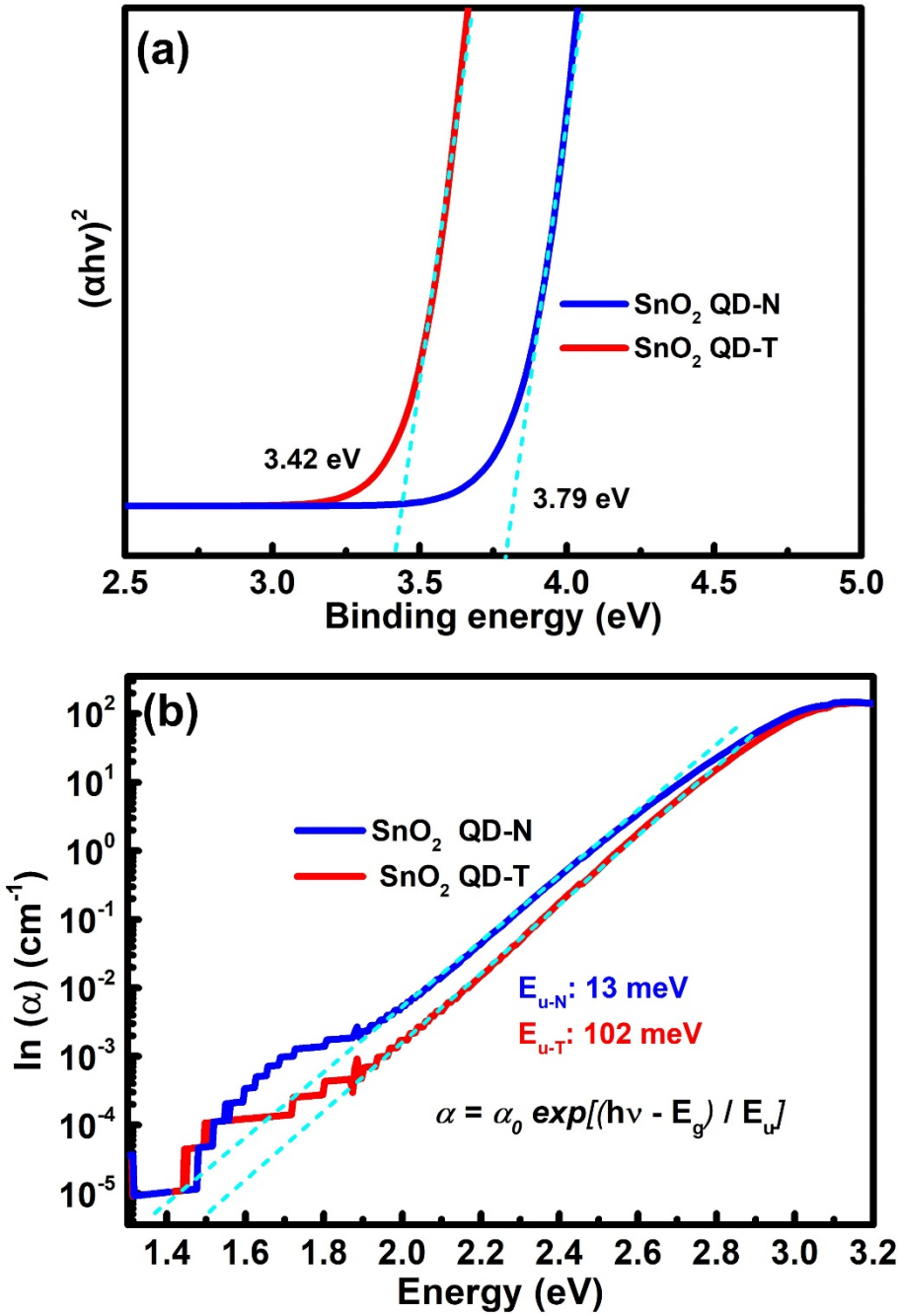

Fig. S7 Urbach energy calculate. (a) Tauc plot $(\alpha h\nu)^2$ vs photon energy and (b) Urbach energy of SnO_2 QDs-N and SnO_2 QDs-T film.

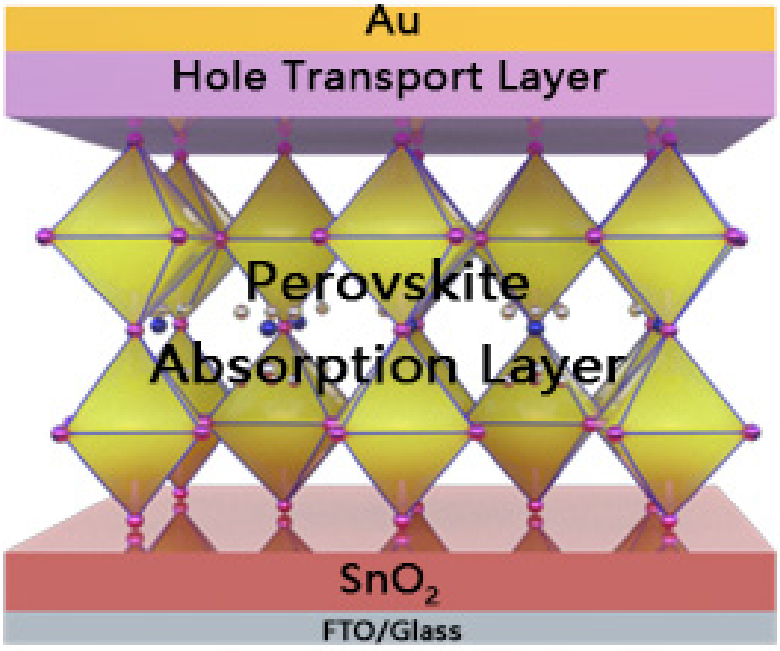

Fig. S8 Schematic structure of PSC device.

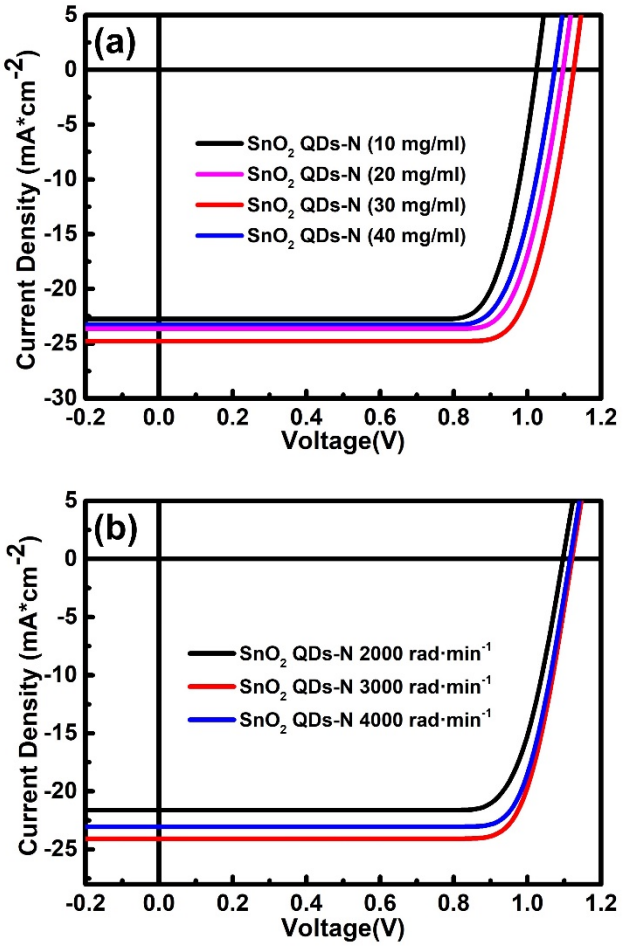

Fig. S9 The J-V curve of PSCs. (a) concentration and (b) speed optimization for SnO_2 QDs-N film.

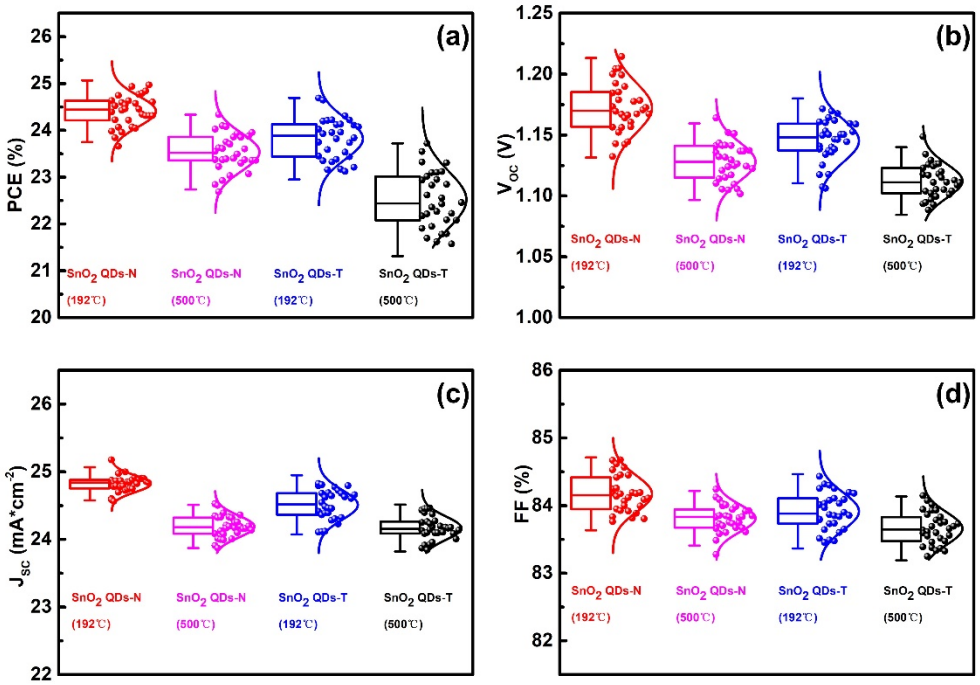

Fig. S10 Performance statistics for each device. (a) *PCE*, (b) V_{oc}, (c) J_{sc} and (d) *FF* statistics of 40 devices for each fabrication condition.

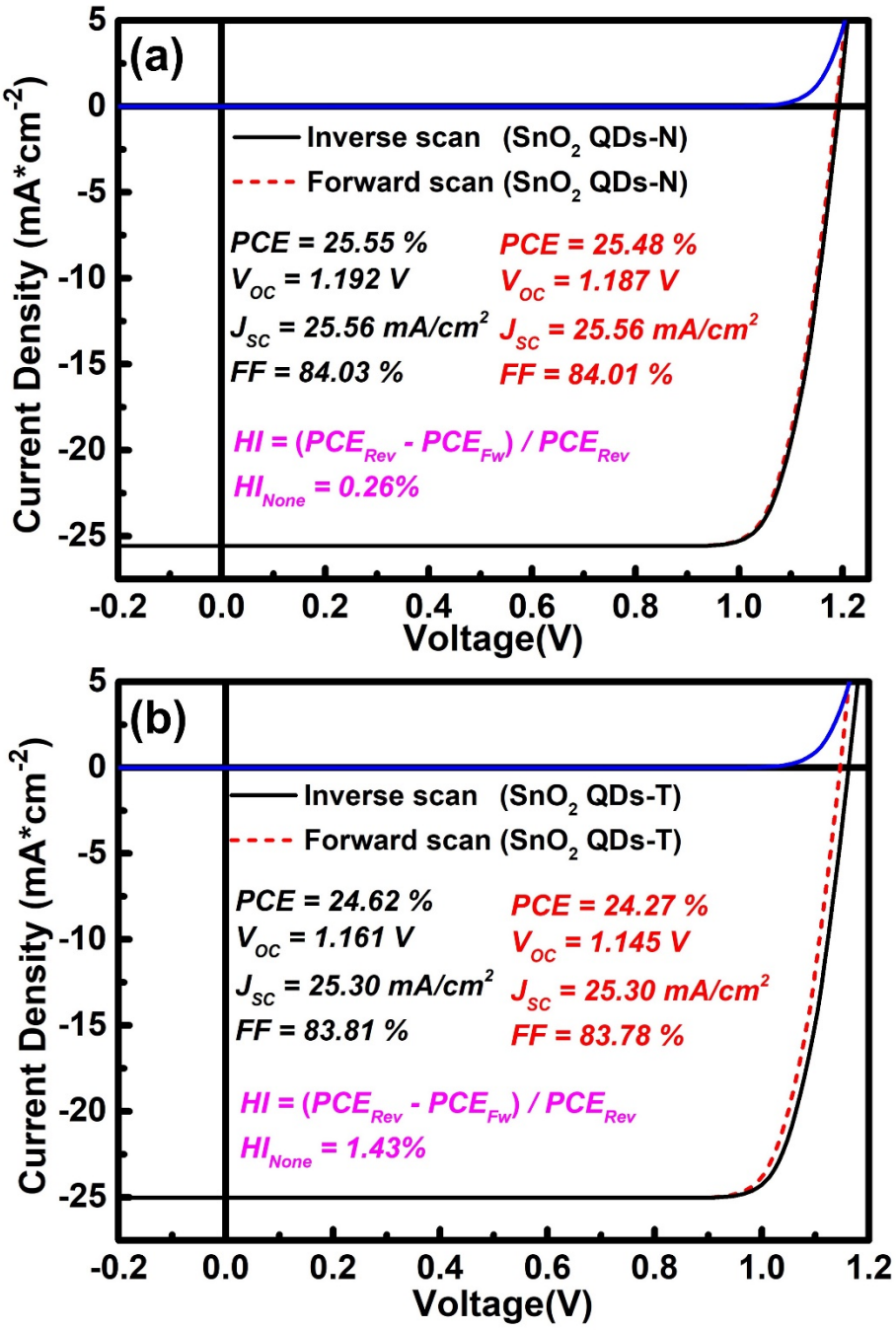

Fig. S11 J-V curve of the champion PSCs device. (a) SnO_2 QDs-N and (b) SnO_2 QDs-T annealed at 192℃.

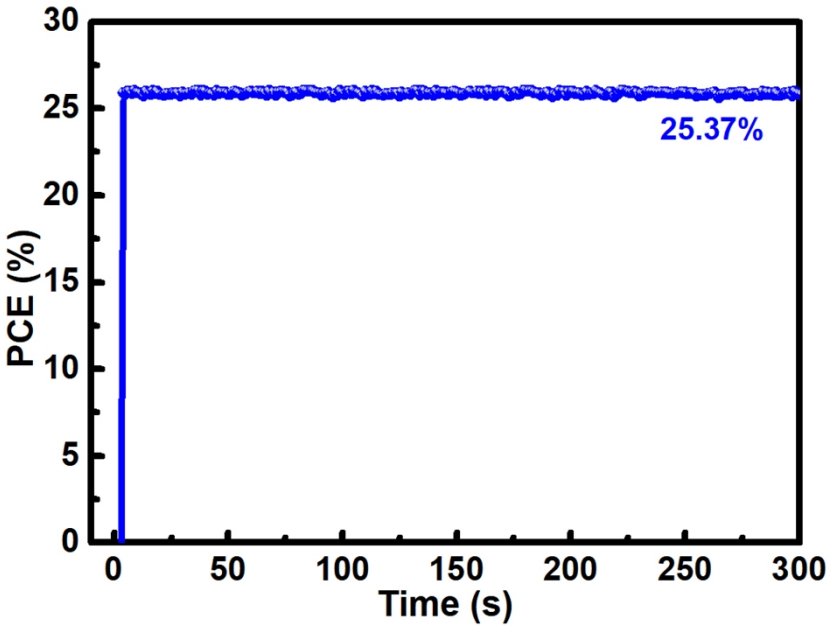

Fig. S12 Steady-state output of the SnO_2 QDs-N PSCs measured at maximum power output point (measured at 1.00 V).

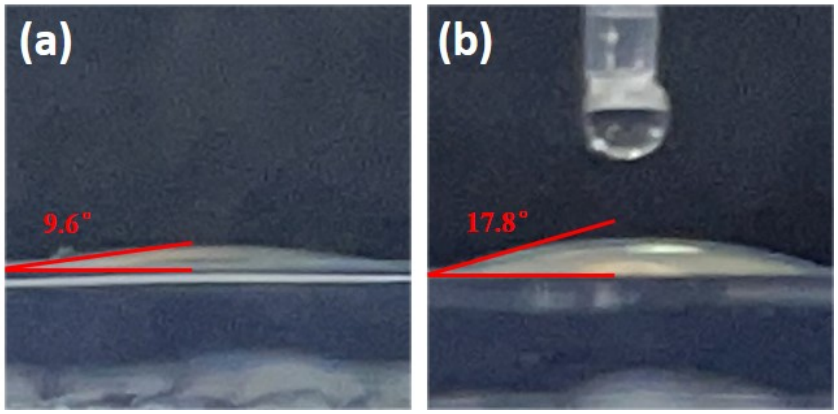

Fig. S13 Water contact angle. (a) SnO_2 QDs-N film and (b) SnO_2 QDs-T film.

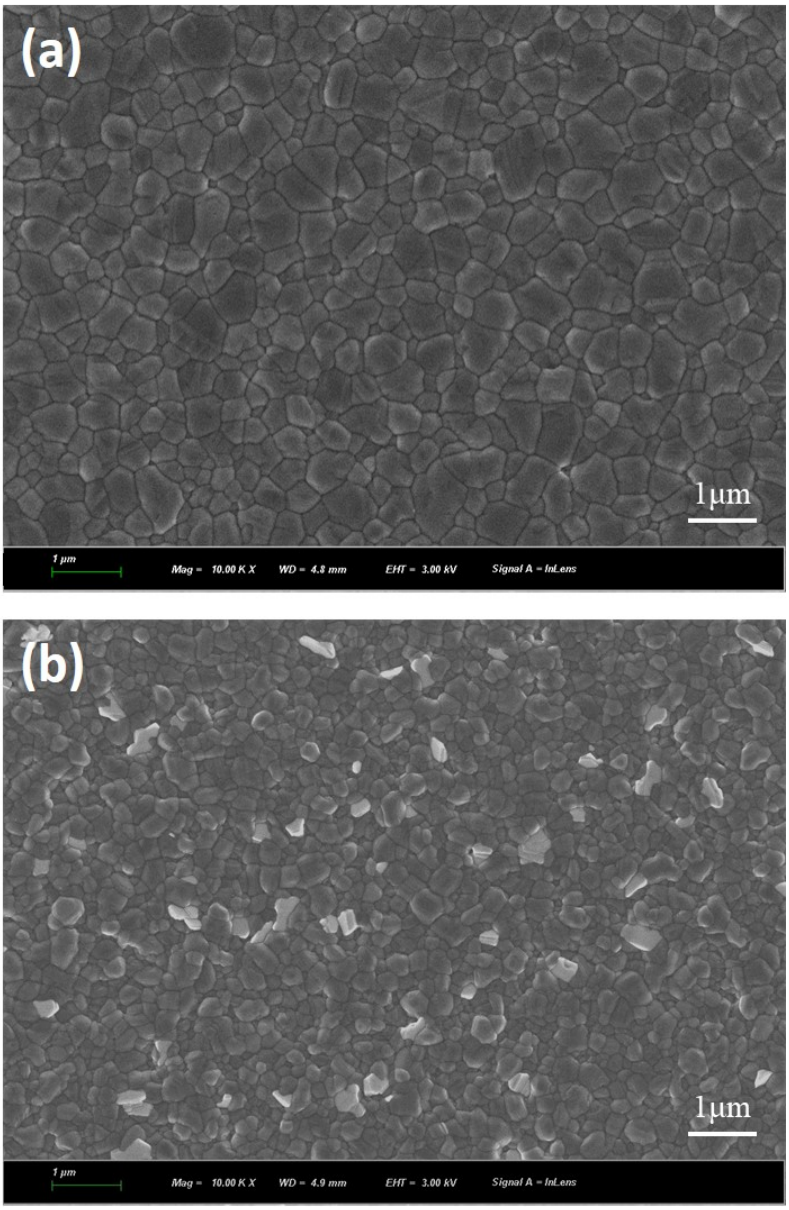

Fig. S14 Surface morphology of perovskite films. SEM images of perovskite on (a) SnO_2 QDs-N and (b) SnO_2 QDs-T film.

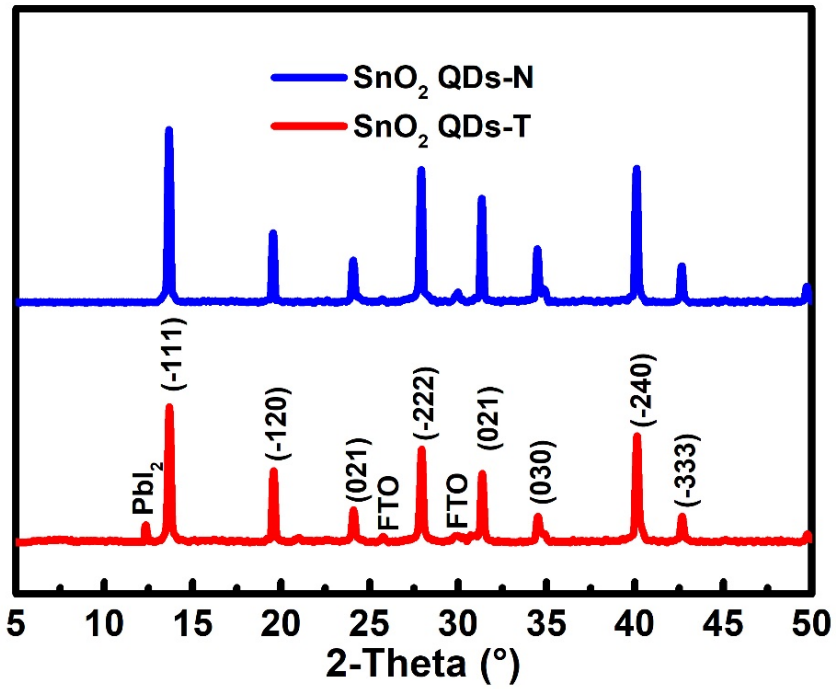

Fig. S15 XRD patterns of perovskite. XRD patterns of perovskite on SnO_2 QDs-N and SnO_2 QDs-T film.

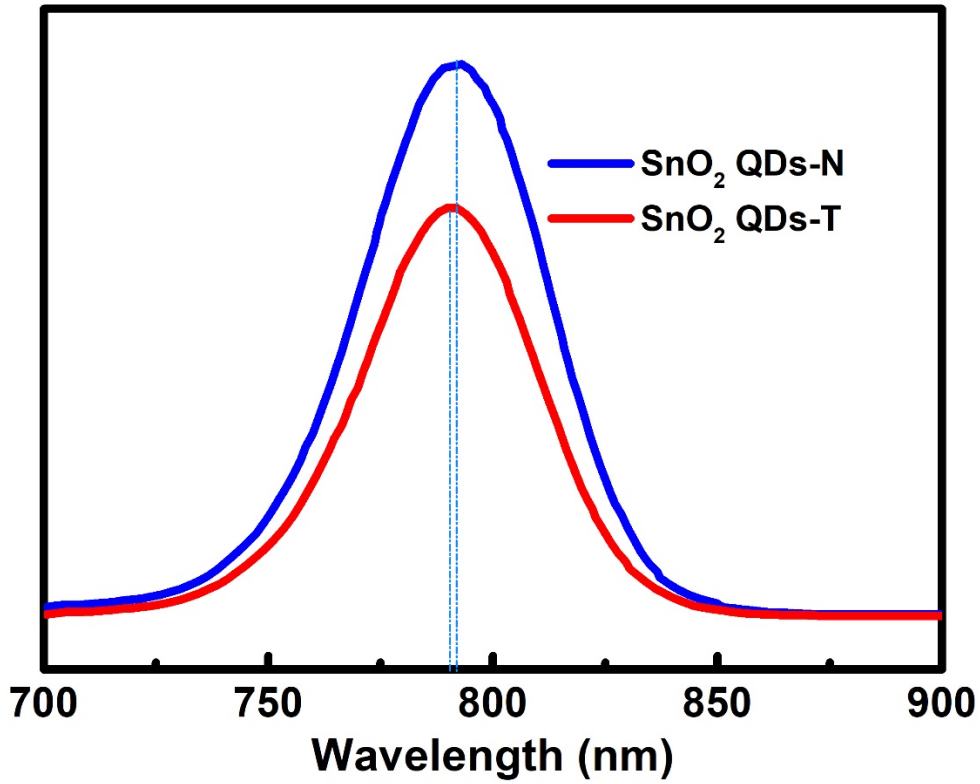

Fig. S16 PL of perovskite. PL of perovskite on SnO_2.

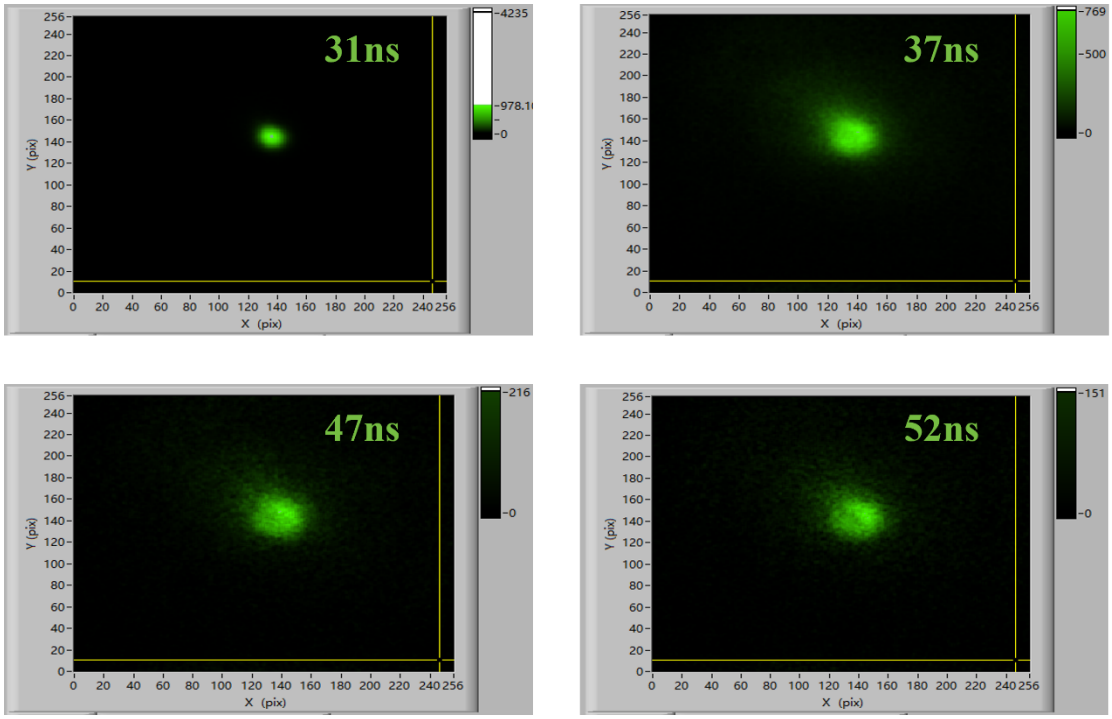

Fig. S17 TPLM images of perovskite. TPLM images of perovskite on SnO_2 QDs-T substrate. Experimental 2D TPLM images of Perovskite film at different delay times of 31, 37, 47, 52 ns.

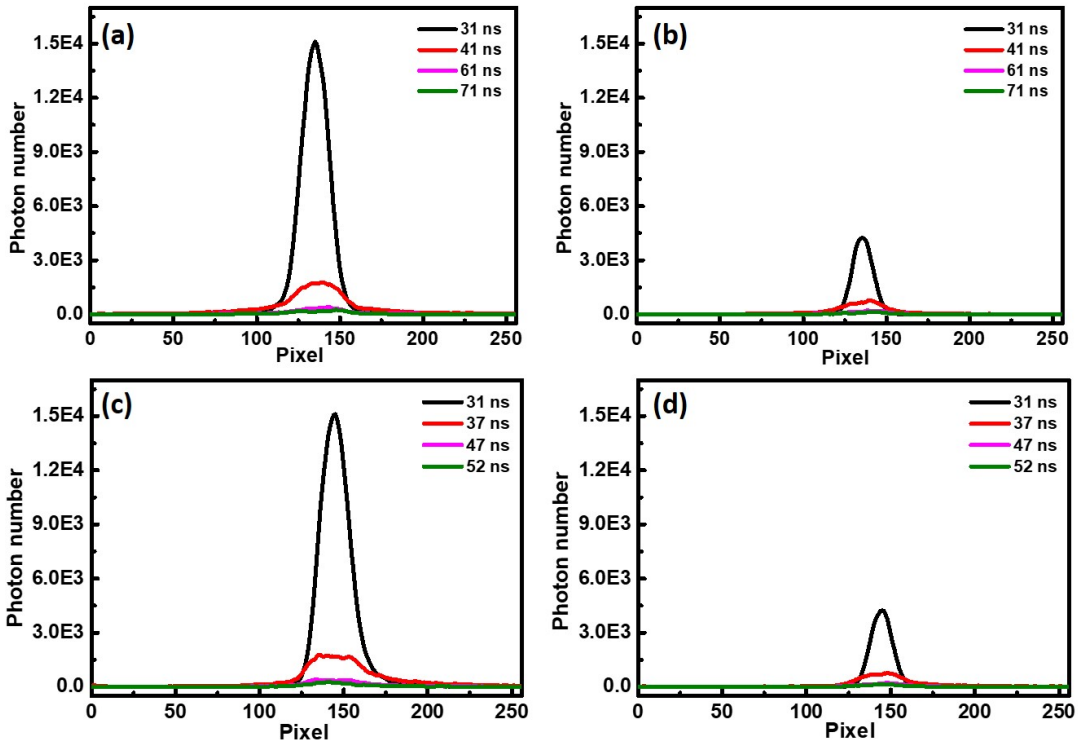

Fig. S18 Photon number extracted from TPLM images. X axis on the (a) SnO_2 QDs-N and (b) SnO_2 QDs-T, Y axis on the (c) SnO_2 QDs-N and (d) SnO_2 QDs-T.

Table S1. The peak position and the composition ratio by XPS. The peak position and the composition ratio of tin valence states in SnO_2 QDs-N and SnO_2 QDs-T from the fitted results of XPS.

Peak position and composition ratio	SnO_2 QDs-N (200℃)	SnO_2 QDs-N (500℃)	SnO_2 QDs-T (200℃)	SnO_2 QDs-T (500℃)
Sn $3d_{5/2}$ (BE eV)	487.2	487.1	487.3	486.3
Sn $3d_{3/2}$ (BE eV)	495.6	495.5	495.8	494.8
$[Sn^{4+}]$/[ALL]	93.3%	97.1%	90.2%	95.1%
$[Sn^{2+}]$/[ALL]	3.5%	2.9%	6.1%	4.9%
$[Sn^{2+}$-Cl]/[ALL]	3.2%	-	3.7%	-

Table S2. Square resistance. The square resistance of SnO_2 QDs-N and SnO_2 QDs-T thin films with annealed at 200℃.

Number of samples	SnO_2 QDs-N (MΩ)	SnO_2 QDs-T (MΩ)
1	25.75	34.76
2	25.36	35.48
3	25.49	37.36
4	25.66	36.04
5	26.18	34.91
6	26.09	37.12
7	25.94	37.65
8	26.37	35.71
Average	25.86	36.13

Table S3 Fitted parameters of TRPL results of perovskite films. Lifetime parameters fitted from fitting curves of the TRPL measurements.

Samples	τ_1 (ns)	A_1 (%)	τ_2 (ns)	A_2 (%)
SnO_2 QDs-N	13.8	13.2	320.1	86.8
SnO_2 QDs-T	24.6	17.1	193.7	82.9

Reference

1. Z. Ren, K. Liu, H. Hu, X. Guo, Y. Gao, P. W. K. Fong, Q. Liang, H. Tang, J. Huang, H. Zhang, M. Qin, L. Cui, H. T. Chandran, D. Shen, M.-F. Lo, A. Ng, C. Surya, M. Shao, C.-S. Lee, X. Lu, F. Laquai, Y. Zhu and G. Li, *Light-Sci Appl.*, 2021, **10**, 239.
2. B. Zhang, Y. Xue, Z. Xue, Z. Li and J. Hao, *ChemPhysChem*, 2015, **16**, 3865-3870.
3. G. Xu, L. Zhang, C. He, D. Ma and Z. Lu, *Sensor Actuat B-Chem.*, 2015, **221**, 717-722.
4. L. Peng, Y. Xie and C. Yang, *RSC Adv.*, 2022, **12**, 5595-5611.
5. J. Chen, H. Dong, J. Li, X. Zhu, J. Xu, F. Pan, R. Xu, J. Xi, B. Jiao, X. Hou, K. W. Ng, S.-P. Wang and Z. Wu, *ACS Energy Lett.*, 2022, **7**, 3685-3694.
6. G. Yang, C. Chen, F. Yao, Z. Chen, Q. Zhang, X. Zheng, J. Ma, H. Lei, P. Qin, L. Xiong, W. Ke, G. Li, Y. Yan and G. Fang, *Adv. Mater.*, 2018, **30**, 1706023.